

SUPPORTING INFORMATION

Tuning the mechanical properties of nanostructured ionomer films by controlling the extents of covalent crosslinking in core-shell nanoparticles

Somjit Tungchaiwattana^a, Robert Groves^b, Peter A. Lovell^a, Orawan Pinprayoon^a and Brian R. Saunders^{a,*}

^aPolymer Science and Technology Group, The School of Materials, The University of Manchester, Grosvenor Street, M1 7HS, UK. ^bSynthomer Ltd, Temple Fields, Harlow, Essex, CM20 2BH, U.K.

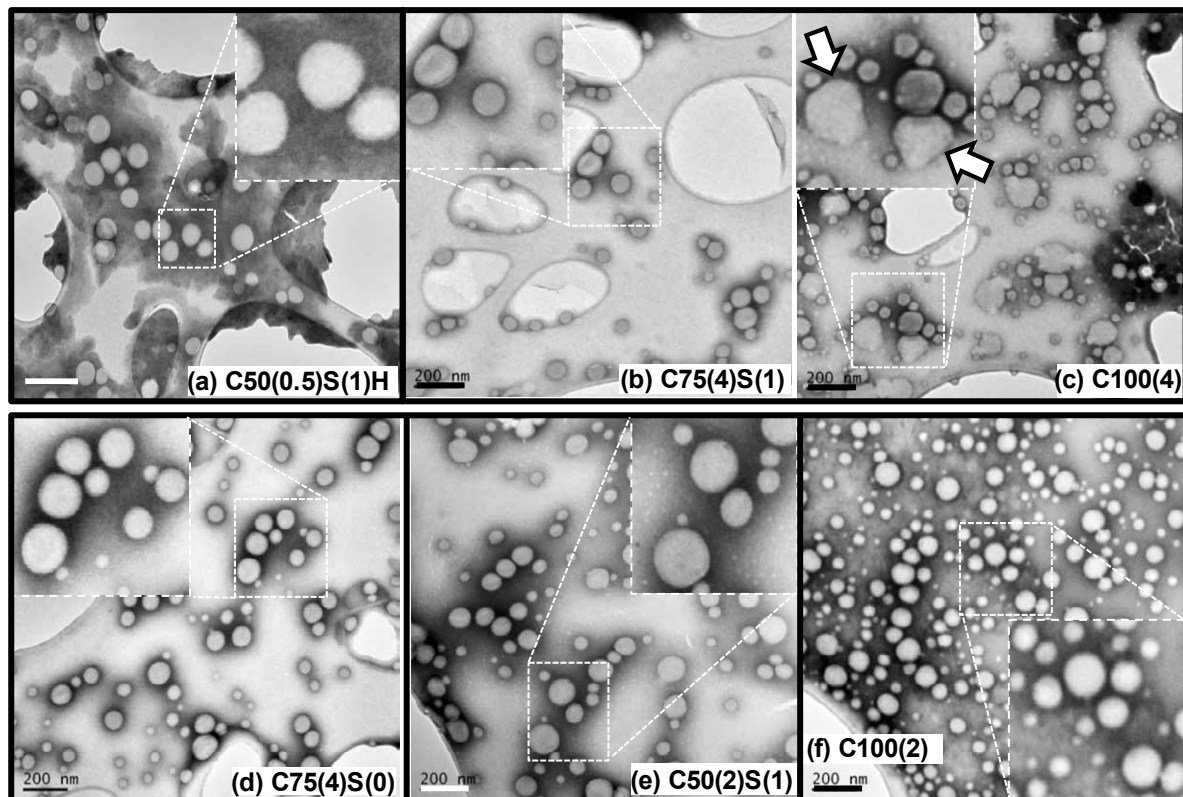


Fig. S1. TEM images of deposited nanoparticles. Their identities are shown in each figure. The arrows in (c) show coalesced nanoparticles. The scale bars are 200 nm.

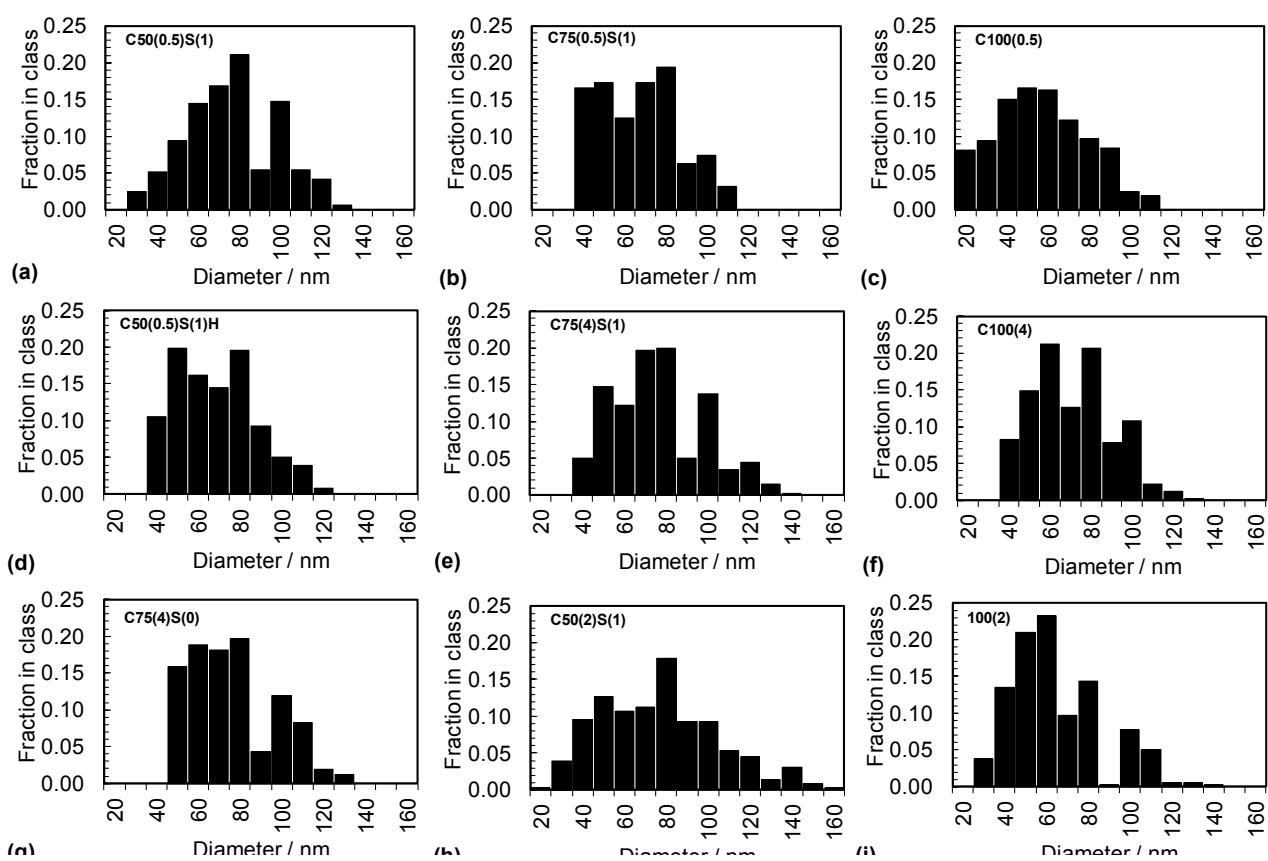


Fig. S2. Particle size distributions for $Cx(y)S(z)$ particles from TEM data.

Table S1: Hydrodynamic diameters for core-shell $Cx(y)S(z)$ and core $C100(y)$ nanoparticles.

Code	d_h^a / nm
C _{50(0.5)} S(1)	110
C ₅₀₍₂₎ S(1)	106
C ₅₀₍₄₎ S(1)	116
C _{50(0.5)} S(1)H	109
C _{75(0.5)} S(1)	104
C ₇₅₍₄₎ S(0)	125
C ₇₅₍₄₎ S(1)	117

C100(0.5)	94
C100(2)	97
C100(4)	102

^a Hydrodynamic diameter measured using PCS.

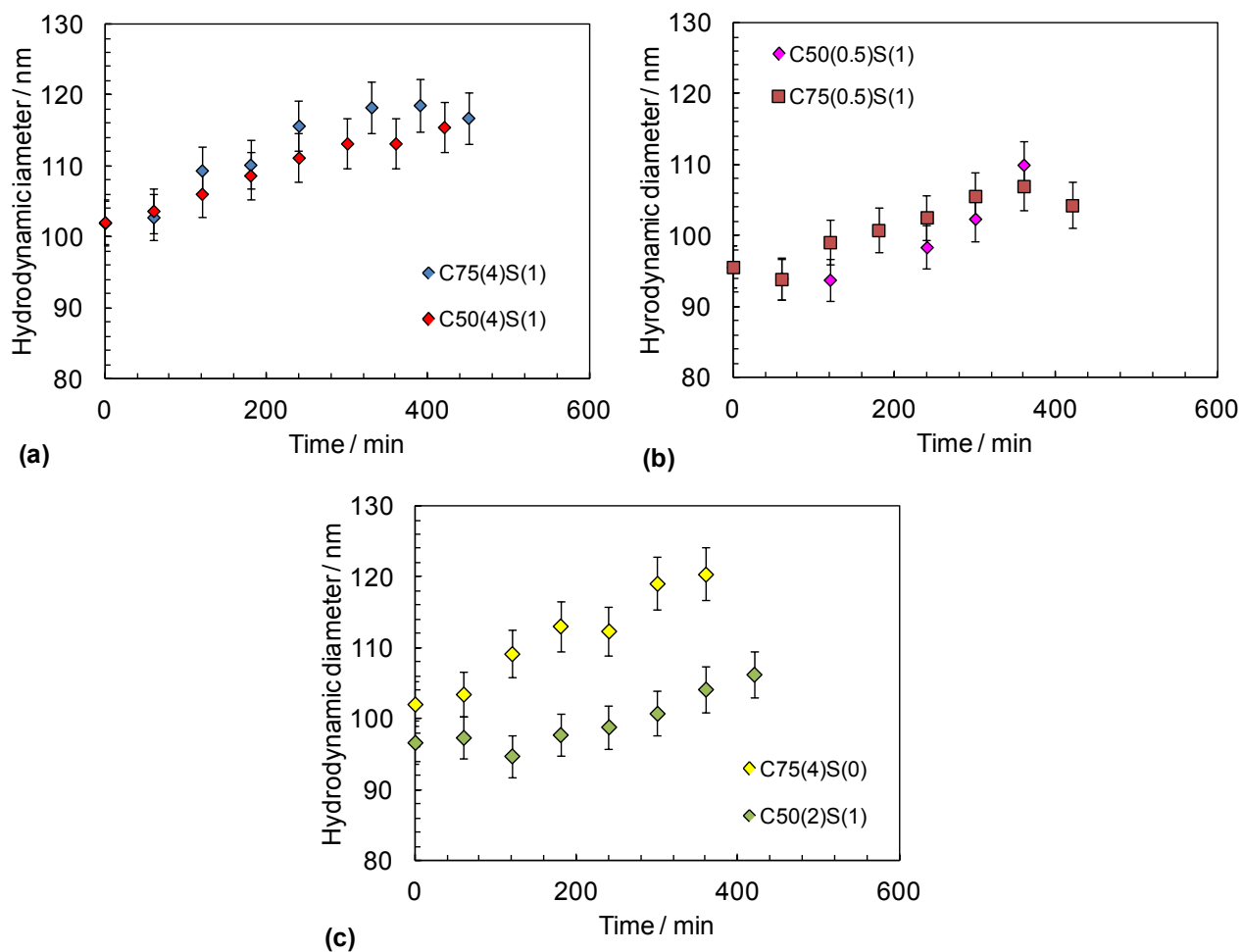


Fig. S3. Variation of hydrodynamic diameter with time for the core-shell systems during shell growth. The error bars are the uncertainty for the data.

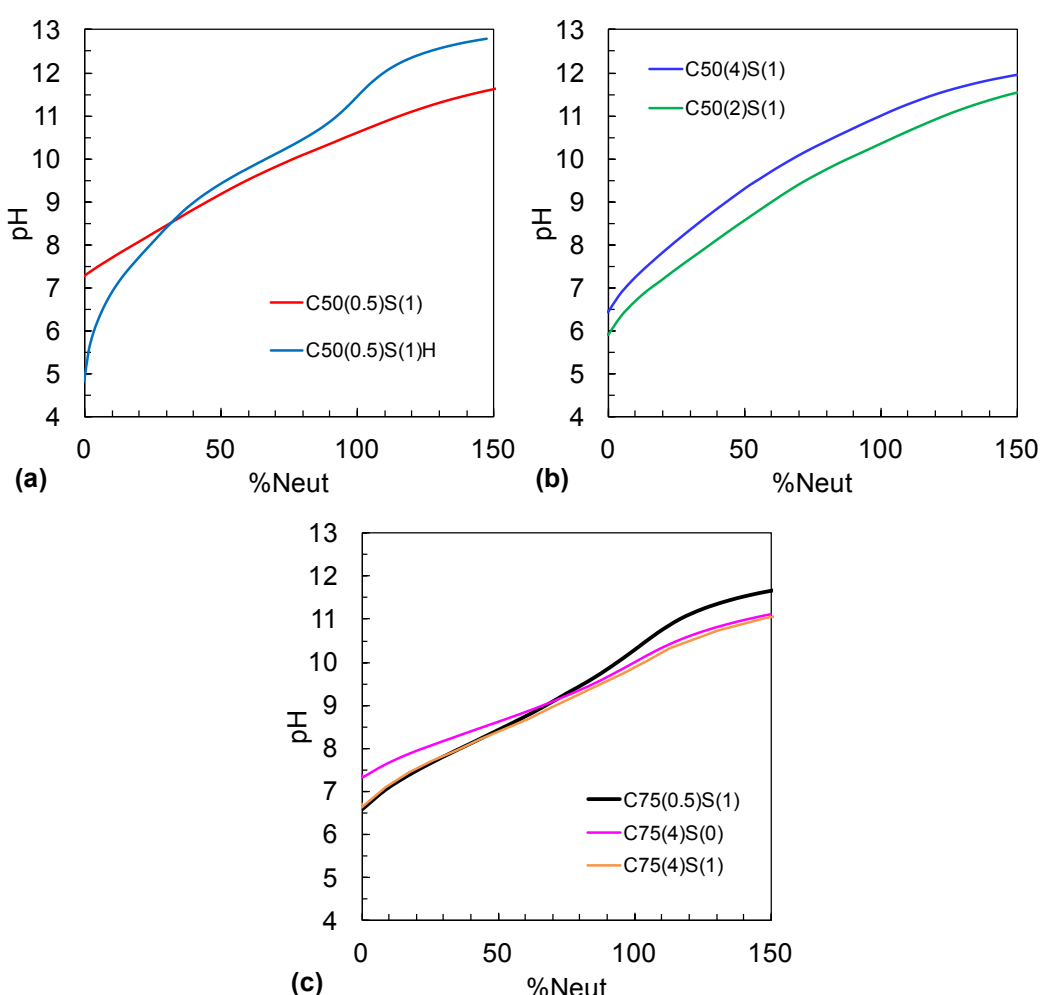


Fig. S4. Titration data for $C_x(y)S(z)$ nanoparticles. The identities are shown in each figure.

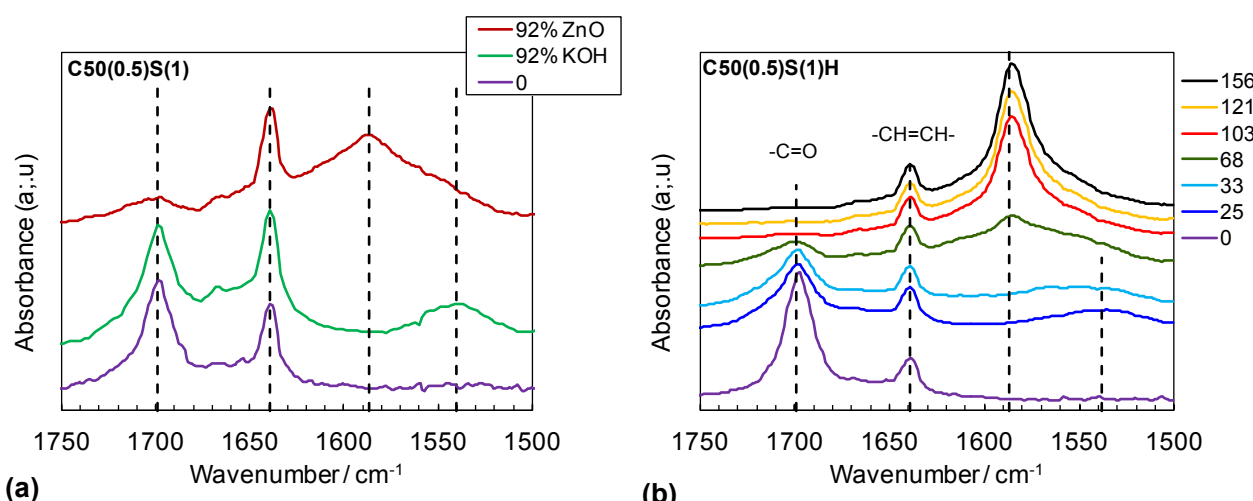


Fig. S5. FTIR spectra of (a) of C₅₀(0.5)S(1) with nominal neutralisations of 92% using KOH or ZnO and (b) C₅₀(0.5)S(1)H films at different nominal neutralisations. The non-neutralised spectrum is also shown for comparison in (a). The absorbance values have been shifted vertically for clarity.

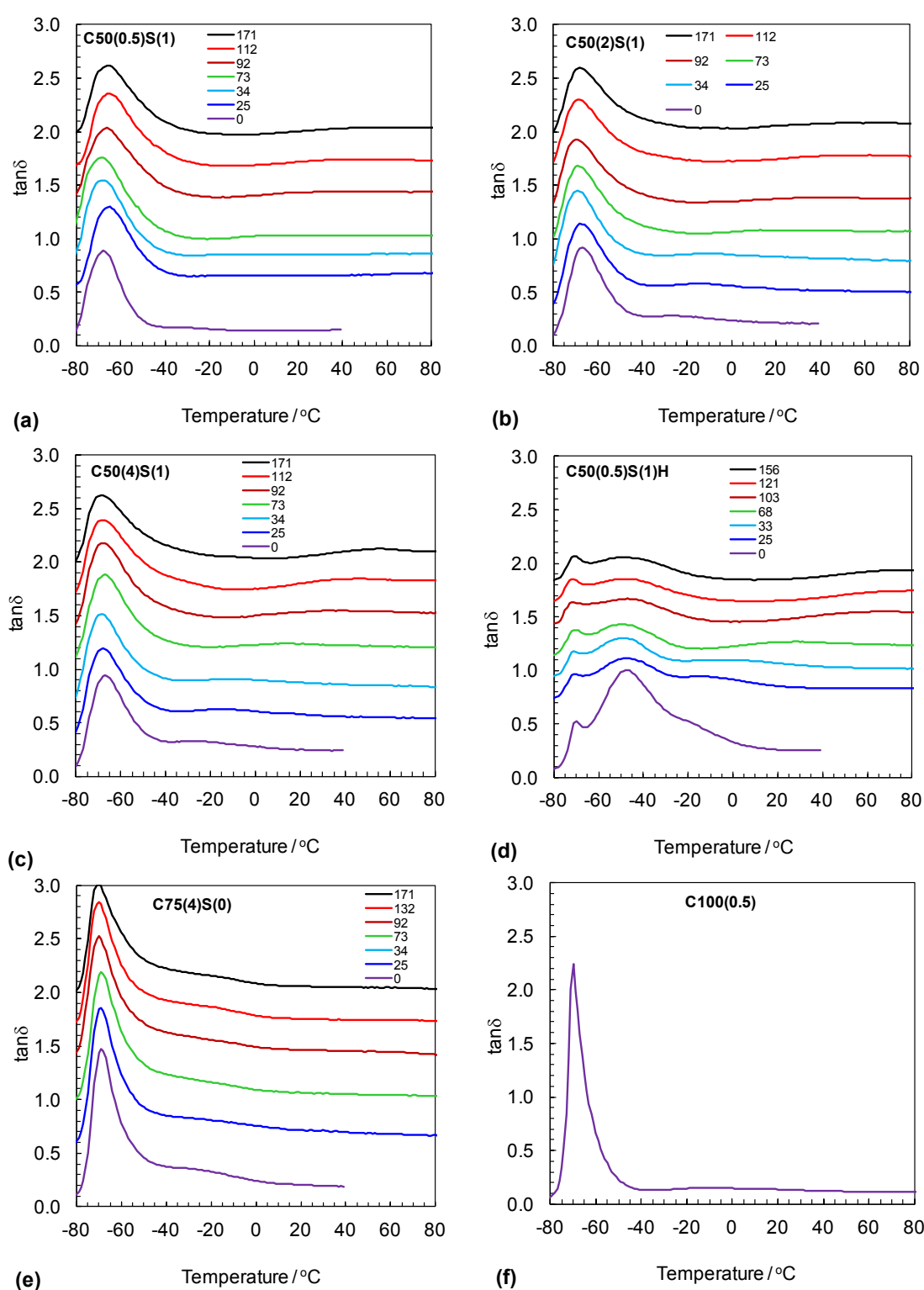


Fig. S6. Variation of $\tan\delta$ with temperature for Cx(y)S(z) films at different nominal neutralisations (α_{nom} , shown in legends). The identity of each film is shown in the graph. The core $\text{C}100(0.5)$ film (f) is also shown for comparison. The $\tan\delta$ data values for $\alpha_{\text{nom}} > 0$ shown in (a) – (e) were offset by adding a factor to the measured $\tan\delta$ values in order to improve clarity.

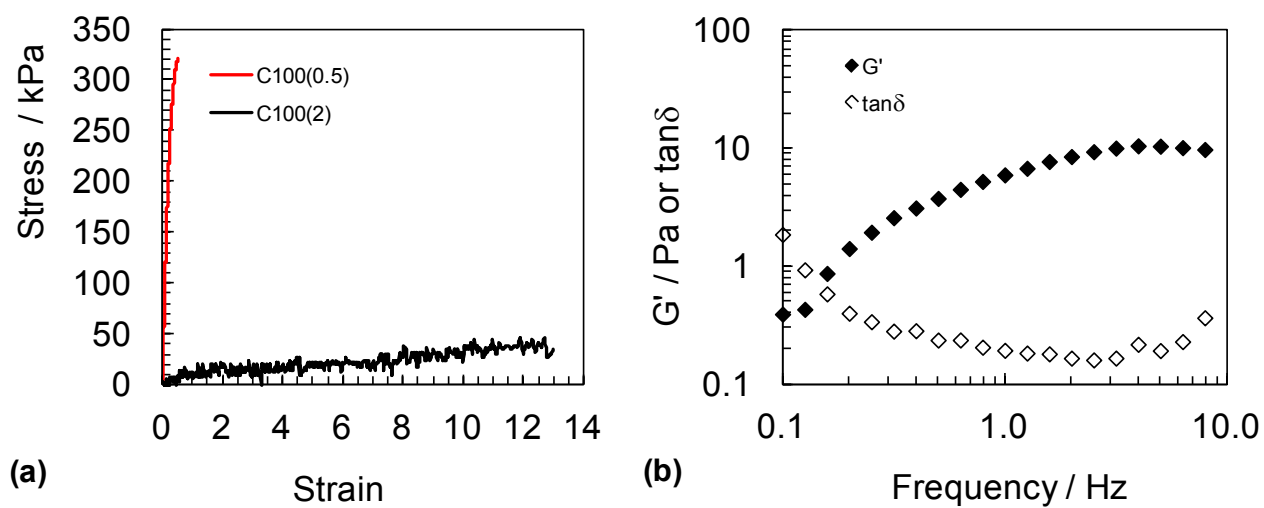


Fig. S7. Mechanical properties of core particle films. (a) Tensile stress vs. strain data C100(0.5) and C100(2) films.
(b) Frequency sweep data for C100(4) films.

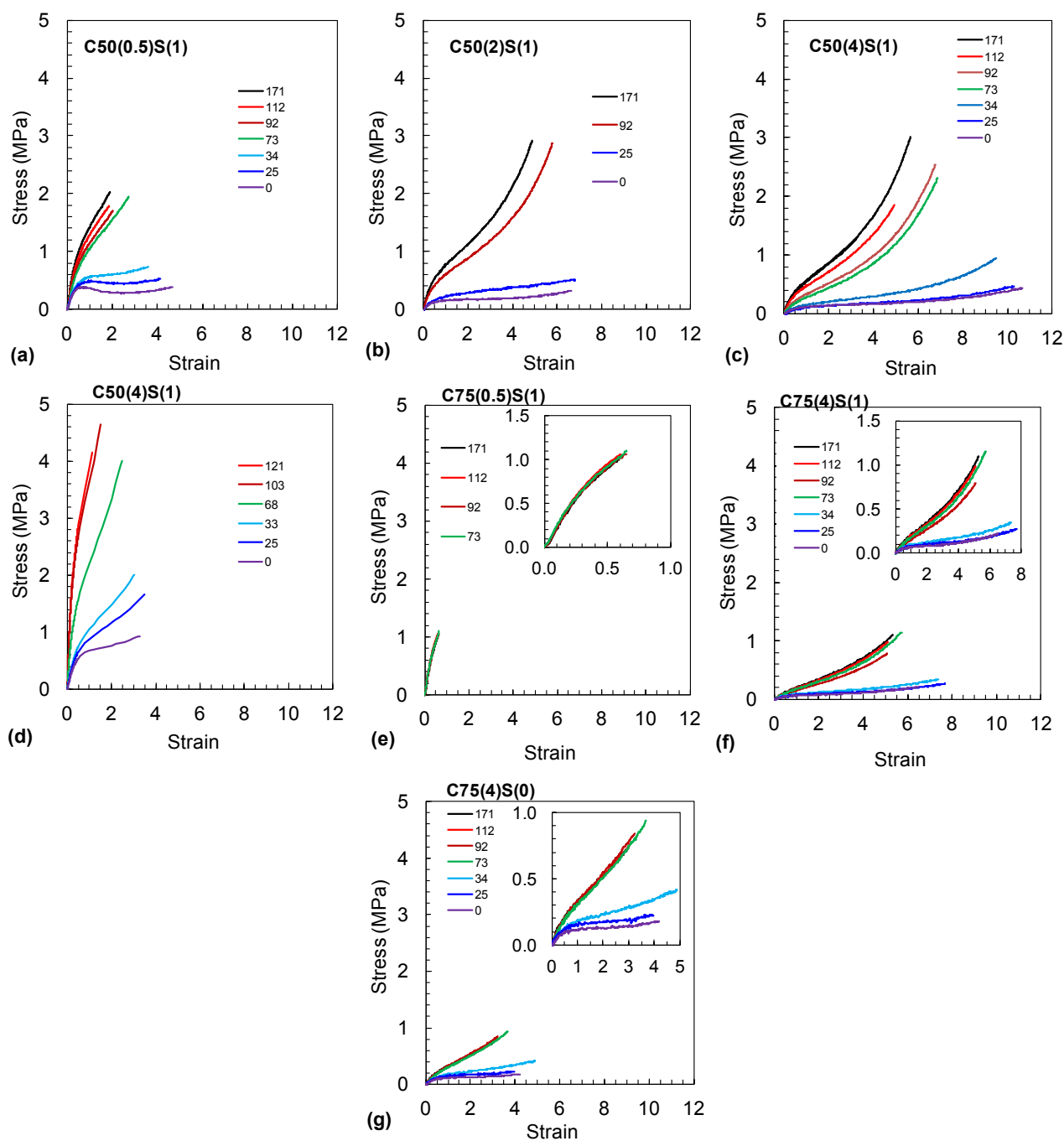


Fig. S8. Stress strain curves for various $C(x)S(y)$ films at different nominal neutralisations (shown in legends). The insets for (e) – (g) show expanded scales.